Therefore, the Lagrange function L is given by

$$L = V_b + V_w - U_b - U_w\,. \tag{A9}$$

According to the Lagrange's motion equation, the dynamic model of an MWIP system can be represented by

$$\begin{aligned}\frac{d}{dt}\left(\frac{\partial L}{\partial \dot{\theta}_b}\right) - \frac{\partial L}{\partial \theta_b} &= -\tau - D_b\left(\dot{\theta}_b - \dot{\theta}_w\right)\\ \frac{d}{dt}\left(\frac{\partial L}{\partial \dot{\theta}_w}\right) - \frac{\partial L}{\partial \theta_w} &= \tau + D_b\left(\dot{\theta}_b - \dot{\theta}_w\right) - D_w\dot{\theta}_w\,.\end{aligned} \tag{A10}$$

It follows from (A10) that the final nonlinear model can be described by (1).

ACKNOWLEDGMENT

The authors would like to thank the Equos Research Co., Ltd. for their help in providing valuable simulation data of a real vehicle.

REFERENCES

[1] K. Pathak, J. Franch, and S. K. Agrawal, "Velocity and position control of a wheeled inverted pendulum by partial feedback linearization," *IEEE Trans. Robot.*, vol. 21, no. 3, pp. 505–513, Jun. 2005.
[2] A. Salerno and J. Angeles, "The control of semi-autonomous two-wheeled robots undergoing large payload-variations," in *Proc. IEEE Int. Conf. Robot. Autom.*, New Orleans, LA, 2004, pp. 1740–1745.
[3] Y.-S. Ha and S. Yuta, "Trajectory tracking control for navigation of the inverse pendulum type self-contained mobile robot," *Robot. Autonom. Syst.*, vol. 17, pp. 65–80, 1996.
[4] Y. Kim, S. H. Kim, and Y. K. Kwak, "Dynamic analysis of a nonholonomic two-wheeled inverted pendulum robot," *J. Intell. Robot. Syst.*, vol. 44, no. 1, pp. 25–46, 2005.
[5] T. J. Ren, T. C. Chen, and C. J. Chen, "Motion control for a two-wheeled vehicle using a self-tuning PID controller," *Control Eng. Practice*, vol. 16, no. 3, pp. 365–375, 2008.
[6] M. Baloh and M. Parent, "Modeling and model verification of an intelligent self-balancing two-wheeled vehicle for an autonomous urban transportation system," presented at the Conf. Comp. Intell., Robot. Autonom. Syst., Singapore, 2003.
[7] F. Grasser, A. D'Arrigo, S. Colombi, and A. Rufer, "Joe: A mobile, inverted pendulum," *IEEE Trans. Ind. Electron.*, vol. 49, no. 1, pp. 107–114, Feb. 2002.
[8] (2010). [Online]. Available: http://www.geology.smu.edu/∼dpa-www/robo/nbot/
[9] (2003). [Online]. Available: http://www.teamhassenplug.org/robots/legway/
[10] H. Tirmant, M. Baloh, L. Vermeiren, T. M. Guerra, and M. Parent, "B2, an alternative two wheeled vehicle for an automated urban transportation system," in *Proc. IEEE Intell. Veh. Symp.*, Paris, France, 2002, pp. 594–603.
[11] (2010). [Online]. Available: http://www.segway.com
[12] M. Karkoub and M. Parent, "Modelling and non-linear feedback stabilization of a two-wheel vehicle," *Proc. Inst. Mech. Eng., I: J. Syst. Control Eng.*, vol. 218, no. 8, pp. 675–686, 2004.
[13] M. W. Spong, "The swing up control problem for the acrobat," *IEEE Control Syst. Mag.*, vol. 15, no. 1, pp. 49–55, Feb. 1995.
[14] I. Fantoni, R. Lozano, and M. W. Spong, "Energy based control of the pendubot," *IEEE Trans. Autom. Control*, vol. 45, no. 4, pp. 725–729, Apr. 2000.
[15] Y.-L. Gu, "Direct adaptive control scheme for underactuated dynamic systems," in *Proc. IEEE Conf. Decision Control*, San Antonio, TX, 1993, pp. 1625–1627.
[16] A. M. Bloch, N. E. Leonard, and J. E. Marsden, "Stabilization of the pendulum on a rotor arm by the method of controlled Lagrangians," in *Proc. IEEE Int. Conf. Robot. Autom.*, Piscataway, NJ, 1999, pp. 500–505.
[17] M. Karkoub, "Modelling and robust μ-synthesis control of an intelligent self balancing two-wheel vehicle," *Proc. Inst. Mech. Eng., K: J. Multi-Body Dyn.*, vol. 220, no. 4, pp. 293–302, 2006.
[18] W. Wang, J. Yi, D. Zhao, and D. Liu, "Design of a stable sliding-mode controller for a class of second-order underactuated systems," *Proc. Inst. Electr. Eng.: Control Theory Appl.*, vol. 151, no. 6, pp. 683–690, 2004.
[19] B. L. Ma, "Comment on 'Design of a stable sliding-mode controller for a class of second-order underactuated systems,'" *IET Control Theory Appl.*, vol. 1, no. 4, pp. 1186–1187, 2007.
[20] H. Ashrafiuon and R. S. Erwin, "Sliding control approach to underactuated multibody systems," in *Proc. Amer. Control Conf.*, Boston, MA, 2004, pp. 1283–1288.
[21] M. Nikkhah, H. Ashrafiuon, and F. Fahimi, "Robust control of underactuated biped using sliding modes," *Robotica*, vol. 25, no. 3, pp. 367–374, 2006.
[22] K. Lee and V. Coverstone-Carroll, "Control algorithms for stabilizing underactuated robots," *J. Robot. Syst.*, vol. 15, no. 12, pp. 681–697, 1998.
[23] C.-Y. Su and Y. Stepanenko, "Sliding mode control of non-holonomic systems: Underactuated manipulator case," in *Proc. Int. Fed. Automat. Control Nonlinear Control Syst. Design*, Tahoe City, CA, 1995, pp. 609–613.
[24] J. Huang, H. W. Wang, T. Matsuno, T. Fukuda, and K. Sekiyama, "Robust velocity sliding mode control of mobile wheeled inverted pendulum systems," in *Proc. IEEE Int. Conf. Robot. Autom.*, Kobe, Japan, 2009, pp. 2983–2988.
[25] A. M. Formal'skii, "An inverted pendulum on a fixed and a moving base," *J. Appl. Math. Mech.*, vol. 70, pp. 56–64, 2006.
[26] O. Matsumoto, S. Kajita, and K. Tani, "Estimation and control of the attitude of a dynamic mobile robot using internal sensors," *Adv. Robot.*, vol. 7, no. 2, pp. 159–178, 1993.

Invariant Trajectory Tracking With a Full-Size Autonomous Road Vehicle

Moritz Werling, Lutz Gröll, and Georg Bretthauer

***Abstract*—Safe handling of dynamic inner-city scenarios with autonomous road vehicles involves the problem of stabilization of precalculated state trajectories. In order to account for the practical requirements of the holistic autonomous system, we propose two complementary nonlinear Lyapunov-based tracking-control laws to solve the problem for speeds between ± 6 m/s. Their designs are based on an extended kinematic one-track model, and they provide a smooth, singularity-free stopping transient. With regard to autonomous test applications, the proposed tracking law without orientation control performs much better with respect to control effort and steering-input saturation than the one with orientation control but needs to be prudently combined with the latter for backward driving. The controller performance is illustrated with a full-size test vehicle.**

***Index Terms*—Back-stepping, full-size autonomous road vehicle, invariant trajectory tracking, Lyapunov-based control, nonholonomic.**

I. INTRODUCTION

The past three decades have witnessed an ambitious research effort in the area of automated driving. This has led to a remarkable enhancement in terms of handling complex situations robustly. The

Manuscript received December 5, 2009; revised April 13, 2010; accepted June 1, 2010. Date of publication July 1, 2010; date of current version August 10, 2010. This paper was recommended for publication by Associate Editor W. Chung and Editor G. Oriolo upon evaluation of the reviewers' comments.

M. Werling is with the Department of Applied Computer Science and Automation, Karlsruhe Institute of Technology, 76128 Karlsruhe, Germany (e-mail: moritz.werling@kit.edu).

L. Gröll and G. Bretthauer are with the Department of Applied Computer Science, Karlsruhe Institute of Technology, 76344 Eggenstein-Leopoldshafen, Germany (e-mail: groell@iai.fzk.de; bretthauer@iai.fzk.de).

This paper has supplementary video material of the test runs available at http://ieeexplore.ieee.org.

Digital Object Identifier 10.1109/TRO.2010.2052325

further autonomous vehicles advance to realistic road traffic the more often they face dynamic, time-critical street scenarios, such as merging into traffic flow, to pass opposing traffic, or to avoid other vehicles. Under simplified conditions, such as during the *2007 DARPA Urban Challenge*,[1] these dynamic scenarios can be tackled with fairly simple heuristics and conservative estimates [14]. However, in nose-to-tail traffic, these approaches quickly reach their limits which results in poor performance or even accidents [3]. This is where genuine trajectory concepts come into play. They explicitly account for the time t on the planning and execution level and, therefore, also allow for a predictable movement that is needed among others in the cooperative maneuvers and safety prognosis.

As a matter of fact, the control of wheeled mobile robots has been, and still is, the subject of numerous research activities (see [9] in combination with [2] and the references therein [8], [13] for a survey). However, to the best of our knowledge, practical implementation of trajectory tracking with full-size road vehicles has yet to be reported. The major challenge of this approach is to deal with the low precision of acceleration and braking commands. On the one hand, it prohibits the direct application of tracking control laws derived for models with velocity-control inputs, which are typical of robots actuated with electrical motors in combination with fast low-level velocity-control loops. On the other hand, the related lateral-tracking errors (not really a safety issue as discussed shortly) question a linearization-based *computed-torque* approach. To avoid these shortcomings, we introduce in Section III a kinematic single-track model with wheel forces as the system's longitudinal input, which bears substantial similarity to a "configuration dynamic model" of type (1,1) in [2]. From there, we propose in Section IV two complementary Lyapunov-based solutions to the trajectory-tracking problem, which represent the main contribution of the paper. Theses solutions exhibit strong analogies with the one proposed in [9] but eliminate substantial practical issues thereof, as will be explained.

Section V briefly describes the implementation of a full-size road vehicle known as *AnnieWAY* from the finals of the *2007 DARPA Urban Challenge* and illustrates its performance data. The results are then discussed in Section VI, which point out the advantages and restrictions of the particular controller. Finally, a short summary and an outlook are given in Section VII.

II. Problem Statement

Similar to [1], we define the problem as follows.

Trajectory tracking: Let $y_d(t) : [0, \infty) \to \mathbb{R}^2$ with $\forall t : \|\dot{y}_d(t)\|_2 \neq 0$ be a given sufficiently smooth time-varying-desired trajectory. Let us design a control law such that all the closed-loop signals are bounded in $\mathcal{L}_\infty$, and the tracking error $\|y(t) - y_d(t)\|_2$ converges for $t \to \infty$ toward zero.

The no-less demanding *fixed-point-stabilization* problem focuses on the previously excluded special case, where $\|\dot{y}_d(t)\|_2 \equiv 0$. Because of the well-known Brockett's theorem, the nonholonomic vehicle model is not asymptotically stabilizable by continuous pure-state feedbacks. Solutions lead to constant shifts in direction, e.g., see [10].

At first glance, it seems feasible to combine one solution of the trajectory-tracking problem with one of the fixed-point stabilization problems to enable the autonomous system to cover the full-speed range. However, tracking controllers with a singularity at $v = 0$ for some t show a fall off in quality, as they merely approach zero velocity, so that they cannot be utilized for the combination. In addition, from the view of the complete autonomous system, a fixed-point controller is not entitled to change the direction constantly, as this should be reserved to the planning level.[2] For these reasons, we search on the one hand for a tracking-control law, which solves the described trajectory-tracking problem. On the other hand, it should allow for a smooth, singularity-free transfer when the desired velocity of the trajectory changes continuously to zero *without* asymptotically stabilizing the final pose. Trajectory planning can then solve the fixed-point-stabilization problem with a scenario-specific sequence of replanned trajectories, according to the accuracy requirements on the final position error.

One approach to avoid the singularity at $v = 0$ in the control law is known as "time-scaling" [12] and has been combined with feedback-linearization methods, such as described in [11]. This method transforms the *complete* system dynamics into a "new time" (either the covered arc length s of the actual or the desired trajectory [11]), for which convergence of the closed-loop system can be shown. Unfortunately, the transformation also unnecessarily includes the longitudinal movement, which leads, in combination with our extended single-track model proposed in Section III, to a new, unremovable singularity.[3] We, therefore, follow [9], which proposes a Lyapunov-based control (assuming velocity as longitudinal input) to avoid the problems associated with $v = 0$ by a conscious design. However, this feedback-law stabilizes not only the lateral and orientational error but *all* states with feedback gains proportional to the desired velocity $v_d(t)$ of the reference trajectory as well. This, in turn, means that the steering angle as well as the longitudinal error when drift v_d (regardless of the actual velocity v) becomes zero. Hence, the proposed control laws do not constitute a suitable start for a back-stepping-based method, which accounts for the wheel force as an input, and therefore, we need to come up with new feedback laws. As discussed in Section V, our approach combines the convergence in s for the lateral and orientational error with the convergence in t for all other states of the closed-loop system.

As the car's dynamics are invariant under the action of the special Euclidean group $SE(2) := SO(2) \times \mathbb{R}^2$, it seems reasonable to search for a "symmetry-preserving" feedback. That is, why should the controlled car act differently when moving south than from when it moves west? A generalization of this idea is referred to as "invariant tracking." For our application, this theory boils down to calculate an invariant error, such as with the Cartan-moving-frame method [8]; see [7].

III. Modeling

The classical kinematic one-track model [2] can be derived under the assumption that the front and rear wheels can be virtually replaced by an intermediate one, which satisfies the "pure rolling" condition. This means that sliding effects are neglected, which holds true for small lateral accelerations typical of low speeds.[4] In this case, the car rotates around its instantaneous center of rotation (ICR),

[1]The DARPA Urban Challenge is a research program conducted in a competitive format to address the challenges of autonomous driving; see http://www.darpa.mil/grandchallenge.

[2]Imagine a four-way stop with a car permanently changing its direction only to keep its position and orientation when waiting for another car.

[3]To stabilize a 2-D chain of integrators $\ddot{x}(t) = u(t)$ along a desired trajectory $x_d(t)$ yields, with $v := \dot{x}$ and $v_d := \dot{x}_d$ in combination with the new time scale $\tau_1(t) = x(t)$ ($\tau_2(t) = x_d(t)$) (required for the removal of the singularity in the lateral dynamics), the time-transformed-differential equation $\mathrm{d}/\mathrm{d}\tau_1[x - x_d] = (v/v_d) - 1$ ($\mathrm{d}/\mathrm{d}\tau_2[x - x_d] = 1 - (v_d/v)$) with a singularity at $v_d = 0$ ($v = 0$). This singularity *cannot* be removed by a control law for u due to the additional integrator of the system that prevents a direct manipulation of v.

[4]According to our experiments, "pure rolling" condition holds up to 6 m/s.

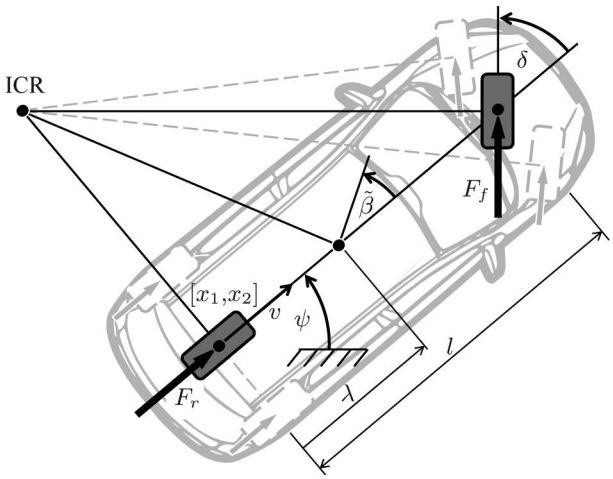

Fig. 1. Nonholonomic car model with longitudinal wheel forces and instantaneous center of rotation.

which depends directly on the orientation of the front and rear wheels, as depicted in Fig. 1. Moreover, the longitudinal velocity v on the rear wheels center $[x_1, x_2]^T$ and the steering angle δ serve as input.

For our application, however, we extend this model so that the steering rate $u_1 = \dot{\delta}$ and the combined longitudinal wheel forces on the front F_f and the rear tires F_r enter the dynamics. As the propulsion of each axis cannot be separately controlled for most of the cars, we introduce the input $u_2 = F = F_f + F_r$ and the ratio $\gamma := F_f/F$. The latter will be considered a two-valued parameter and depends on the car design, as will be discussed in Section III. With the total vehicle mass m, the distance l_{CoG} of the center of gravity to the rear axis, the vehicle moment of inertia J_{CoG}, the short notation $M := (ml_{\mathrm{CoG}}^2 + J_{\mathrm{CoG}})/l^2$, and the notion of Fig. 1, by the use of Lagrangian mechanics, the total system equations are provided by

$$\begin{bmatrix} \dot{x}_1 \\ \dot{x}_2 \\ \dot{\psi} \\ \dot{\delta} \\ \dot{v} \end{bmatrix} = \begin{bmatrix} v\cos\psi \\ v\sin\psi \\ v\dfrac{\tan\delta}{l} \\ u_1 \\ \dfrac{\left[1+\gamma\left[\frac{1}{\cos\delta}-1\right]\right]u_2 - 2Mv\frac{\tan\delta}{\cos^2\delta}u_1}{m+M\tan^2\delta} \end{bmatrix}. \tag{1}$$

As the system's generic output, we use the position of a point

$$\tilde{y} = \begin{bmatrix} \tilde{y}_1 \\ \tilde{y}_2 \end{bmatrix} = \begin{bmatrix} x_1 \\ x_2 \end{bmatrix} + \lambda \begin{bmatrix} \cos\psi \\ \sin\psi \end{bmatrix} \tag{2}$$

on the longitudinal axis of the car with a distance λ from the rear wheel center toward the front. In the following, all variables denoted with $\tilde{()}$ refer to this point, and the ones without to the rear-axis center with $\lambda = 0$. Notice that, it can be easily shown that our input extension has not changed the flatness property[5] [4] of the system.

[5]Flat systems have a, possibly fictitious, flat output, which can be used to explicitly express all states and inputs in terms of the flat output and a finite number of its derivatives.

IV. Nonlinear Tracking Control

A. Trajectory Representation

Clearly, the trajectory-planning level has to continuously specify both the position and the orientation for a collision-free movement toward the destination. Therefore, it is reasonable to parameterize the desired trajectory in terms of the flat output y given by (2) with $\lambda = 0$, as it completely describes the desired values of all system states [4]. While jerk-optimal trajectories provide a pleasant ride, the desired trajectory does not have to be of a special type. As long as it is sufficiently smooth and accounts for the limited turn radius and steering rate of the car, we will be able to stabilize it. Nonadmissible trajectories (see [10]) are not considered here, as they do not meet our notion of a coherent coaction between trajectory-planning and stabilization. To simplify calculations, we introduce the desired tracking direction $\varsigma \in \{-1, 1\}$, -1 for reverse and 1 for forward driving, and the short notation

$$v_d := \varsigma\dot{s}_d = \varsigma\sqrt{\dot{y}_{d1}^2 + \dot{y}_{d2}^2}, \quad \psi_d := \operatorname{atan2}\left(\varsigma\dot{y}_{d2}, \varsigma\dot{y}_{d1}\right), \quad \kappa_d := \frac{\dot{\psi}_d}{v_d}$$

for the desired trajectory $y_d(t)$. Notice that $\dot{s}_d \geq 0$ for both forward and backward driving.

B. Longitudinal Input Substitution

Throughout the paper, we assume that the measurement values of all states are available so that we can introduce

$$w_2 := \frac{\left[1+\gamma\left[\frac{1}{\cos\delta}-1\right]\right]u_2 - 2Mv\frac{\tan\delta}{\cos^2\delta}u_1}{m+M\tan^2\delta} = \dot{v} \tag{3}$$

as suggested in [9], which represents a new virtual-system input for the subsequently proposed control laws. As long as $|\delta| < \pi/2$, these laws can certainly be rewritten for the original control variable, since $u_2 \mapsto w_2$ given by (3) is a bijective mapping for a known steering input u_1 with the inverse function

$$u_2 = \frac{1}{1+\gamma\left[\frac{1}{\cos\delta}-1\right]}\left[w_2[m+M\tan^2\delta] + 2Mv\frac{\tan\delta}{\cos^2\delta}u_1\right].$$

For the sake of conciseness, all input substitutions described in the following imply this procedure.

C. Asymptotical Trajectory Tracking With Orientation Control

For a start, let $\lambda = 0$. Let us consider the global diffeomorphic-coordinate transformation

$$\begin{bmatrix} e_t \\ e_n \\ e_\psi \\ v \\ \kappa_\delta \end{bmatrix} := \begin{bmatrix} \begin{bmatrix} \cos\psi_d & \sin\psi_d \\ -\sin\psi_d & \cos\psi_d \end{bmatrix}\begin{bmatrix} y_1 - y_{1d} \\ y_2 - y_{2d} \end{bmatrix} \\ \psi - \psi_d \\ v \\ \dfrac{\tan\delta}{l} \end{bmatrix} \tag{4}$$

that transforms the tracking error to a Frenet frame, as depicted in Fig. 2. This step provides the invariance property of the closed-loop system, as already mentioned earlier.

Taking the derivative and applying the input substitution (3), the system (1) becomes

$$\dot{e}_t = v\cos e_\psi - v_d[1 - \kappa_d e_n] \tag{5a}$$

$$\dot{e}_n = v\sin e_\psi - v_d\kappa_d e_t \tag{5b}$$

$$\dot{e}_\psi = v\,\kappa_\delta - v_d\kappa_d \tag{5c}$$

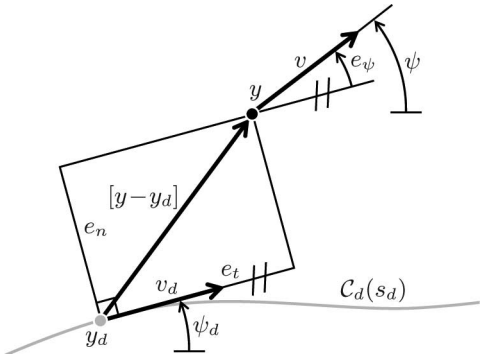

Fig. 2. Definition of the scalar-invariant tracking errors.

$$\dot{v} = w_2 \tag{5d}$$

$$\dot{\kappa}_\delta = \left[\frac{1}{l} + l\kappa_\delta^2\right] u_1 . \tag{5e}$$

Pretending (5e) does not exist and manipulating κ_δ in (5c) directly by a control law ξ_1 so that $\kappa_\delta = \xi_1$, we propose the following:

Lemma 1: The control law for the fictitious input κ_δ and the virtual input w_2 given by

$$\xi_1 = \kappa_d - k_1 \left[e_t \frac{\cos e_\psi - 1}{e_\psi} + e_n \frac{\sin e_\psi}{e_\psi} \right] - \varsigma k_2 e_\psi \tag{6}$$

$$w_2 = \dot{v}_d - k_1 e_t - k_3 e_v + \varsigma k_2 e_\psi^2 - e_\psi \kappa_d \tag{7}$$

with $e_v := v - v_d$, $k_1, k_2, k_3 > 0$ renders $[e_t, e_n, e_\psi, e_v] = 0$ of the truncated system (5a)–(5d) for $\dot{s}_d \neq 0$ asymptotical stable.

Proof: Time derivative of the Lyapunov function candidate

$$V = \frac{1}{2}\left[k_1 e_t^2 + k_1 e_n^2 + e_\psi^2 + e_v^2\right] \tag{8}$$

yields

$$\begin{aligned}
\dot{V} &= k_1 e_t \dot{e}_t + k_1 e_n \dot{e}_n + e_\psi \dot{e}_\psi + e_v \dot{e}_v \\
&= k_1 e_t [v \cos e_\psi - v_d [1 - \kappa_d e_n]] + k_1 e_n [v \sin e_\psi - v_d \kappa_d e_t] \\
&\quad + e_\psi [v \xi_1 - v_d \kappa_d] + e_v [w_2 - \dot{v}_d] \\
&= k_1 e_t [v \cos e_\psi - v_d [1 - \kappa_d e_n]] + k_1 e_n [v \sin e_\psi - v_d \kappa_d e_t] \\
&\quad + e_\psi v \left[\kappa_d - k_1 \left[e_t \frac{\cos e_\psi - 1}{e_\psi} + e_n \frac{\sin e_\psi}{e_\psi} \right] - \varsigma k_2 e_\psi \right] \\
&\quad - e_\psi v_d \kappa_d + e_v [-k_1 e_t - k_3 e_v + k_2 \varsigma e_\psi^2 - e_\psi \kappa_d] \\
&= k_1 e_t [v - v_d] - \varsigma k_2 e_\psi^2 v + e_v [-k_1 e_t - k_3 e_v + \varsigma k_2 e_\psi^2] \\
&= -\varsigma v_d k_2 e_\psi^2 - k_3 e_v^2 = -\dot{s}_d k_2 e_\psi^2 - k_3 e_v^2 \leq 0.
\end{aligned}$$

As the derivative $\dot{V}$ is negative semidefinite, we can only conclude that $[e_t, e_n, e_\psi, e_v] = 0$ is stable. In order to prove asymptotical stability, we apply LaSalle's invariance theorem [6].

Let $S = \{[e_t, e_n, e_\psi, e_v] \,|\, \dot{V} = 0\}$. With $\dot{V} = 0$, we conclude $e_\psi \equiv 0$; $e_v \equiv 0$, and therefore, with $\kappa_\delta = \xi_1$, one gets

$$e_v \equiv 0 \Rightarrow \dot{e}_v \equiv 0 \Rightarrow \dot{v} = \dot{v}_d \overset{(5d),(7)}{\Rightarrow} e_t = 0 \tag{9}$$

$$e_\psi \equiv 0 \Rightarrow \dot{e}_\psi \equiv 0 \overset{(5c)}{\Rightarrow} \kappa_d = \kappa_\delta = \xi_1 \overset{(6)}{\Rightarrow} e_n = 0. \tag{10}$$

Therefore, the only solution that can stay identical in the set S is $[e_t, e_n, e_\psi, e_v] = 0$. ■

As the system (5) has already been transformed to strict-feedback form, we can shortly follow standard back-stepping procedure [6] to account for the real system input u_1. Introducing the new input $w_1 := \dot{\kappa}_\delta$ and pursuing a change of variables

$$e_\delta := \kappa_\delta - \xi_1 \tag{11}$$

we propose the following theorem,

Theorem 1: The control law for the virtual input w_1 given by

$$w_1 = -e_\psi v + \dot{\xi}_1 - k_4 e_\delta \tag{12}$$

$$\begin{aligned}
\text{with} \quad \dot{\xi}_1 = \dot{\kappa}_d - k_1 \Bigg[& \dot{e}_t \frac{\cos e_\psi - 1}{e_\psi} + e_t \dot{e}_\psi \frac{\mathrm{d}}{\mathrm{d}e_\psi} \left[\frac{\cos e_\psi - 1}{e_\psi} \right] \\
& + \dot{e}_n \frac{\sin e_\psi}{e_\psi} + e_n \dot{e}_\psi \frac{\mathrm{d}}{\mathrm{d}e_\psi} \left[\frac{\sin e_\psi}{e_\psi} \right] \Bigg] - \varsigma k_2 \dot{e}_\psi
\end{aligned} \tag{13}$$

and $k_4 > 0$, combined with the stabilization (7) renders $[e_t, e_n, e_\psi, e_v, e_\delta] = 0$ of the system (5) for $\dot{s}_d \neq 0$ asymptotical stable.

Proof: Time derivative of (11) yields the transformed system equation $\dot{e}_\delta = w_1 - \dot{\xi}_1$. Taking $V_c = V + (1/2)e_\delta^2$ as a composite Lyapunov-function candidate, we get

$$\begin{aligned}
\dot{V}_c &= \dot{V} + e_\delta \dot{e}_\delta \\
&= k_1 e_t [v \cos e_\psi - v_d [1 - \kappa_d e_n]] + k_1 e_n [v \sin e_\psi - v_d \kappa_d e_t] \\
&\quad + e_\psi [v [\xi_1 + e_\delta] - v_d \kappa_d] + e_v [w_2 - \dot{v}_d] + e_\delta [w_1 - \dot{\xi}_1] \\
&= -\dot{s}_d k_2 e_\psi^2 - k_3 e_v^2 + e_\delta [e_\psi v + w_1 - \dot{\xi}_1]
\end{aligned}$$

so that with (12) and Lemma 1

$$\dot{V}_c = -\dot{s}_d k_2 e_\psi^2 - k_3 e_v^2 - k_4 e_\delta^2 \leq 0.$$

For asymptotic stability, we conclude from $\dot{V}_c = 0$ that $e_\delta \equiv 0$, and with (11), we get that $\kappa_\delta = \xi_1$. Therefore, (9) and (10) still hold, and we deduce that the only solution that can stay identical in the set $S_c = \{[e_t, e_n, e_\psi, e_v, e_\delta] \,|\, \dot{V}_c = 0\}$ is $[e_t, e_n, e_\psi, e_v, e_\delta] = 0$. ■

Notice that in (12) and in the following section, the expressions $[\cos e_\psi - 1]/e_\psi$ and $\sin e_\psi / e_\psi$, as well as their derivatives in (13), have removable singularities and can be implemented sufficiently accurately[6] by their Taylor series approximations.

D. Asymptotical Trajectory Tracking Without Orientation Control

As the controller for the flat output stabilizes the rear-axis center along its desired trajectory, it is not surprising due to the long lever that the front tilts unintentionally out, whenever the controller needs to correct. As a matter of fact, we are interested in stabilizing the car so that it remains close to the previously determined collision-free configuration. Therefore, it is valid to ask for a controller, which stabilizes the car center directly.

We now chose $\lambda \approx \frac{l}{2} > 0$ so that the position $\tilde{y}$ of the vehicle's geometric center is our system output. As trajectory-generation methods are usually based on the choice between numerous alternative trajectories, collision checking to account for the vehicle's orientation has to be fast. In order to avoid solving (numerically) the zero dynamics for each potential trajectory to get the orientation in each time step, we keep planning for the flat output with $\lambda = 0$. Therefore, the straightforward transformation $y_d(t) \mapsto \tilde{y}_d(t)$ (see Fig. 3) to provide the desired course angle $\tilde{\theta}_d$ and curvature $\tilde{\kappa}_d$ needs to be pursued first.

[6]We use seventh- and eight-order polynomials.

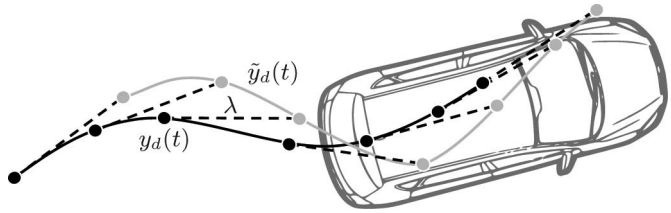

Fig. 3. Transformation of the desired trajectory from the rear-axis center $y_d(t)$ to the geometric vehicle center $\tilde{y}_d(t)$.

With the new course angle error $\tilde{e}_\theta = [\psi + \tilde{\beta}] - \tilde{\theta}_d$, the analog to (4) is chosen as

$$\begin{bmatrix} \tilde{e}_t \\ \tilde{e}_n \\ \tilde{e}_\theta \\ \tilde{v} \\ \tilde{\beta} \end{bmatrix} := \begin{bmatrix} \begin{bmatrix} \cos\tilde{\theta}_d & \sin\tilde{\theta}_d \\ -\sin\tilde{\theta}_d & \cos\tilde{\theta}_d \end{bmatrix} \begin{bmatrix} \tilde{y}_1 - \tilde{y}_{1d} \\ \tilde{y}_2 - \tilde{y}_{2d} \end{bmatrix} \\ \psi + \arctan\left(\dfrac{\lambda}{l}\tan\delta\right) - \tilde{\theta}_d \\ v\sqrt{1 + \left[\dfrac{\lambda}{l}\right]^2 \tan^2\delta} \\ \arctan\left(\dfrac{\lambda}{l}\tan\delta\right) \end{bmatrix}. \tag{14}$$

With the input substitution (3), the invariant dynamics can be found as

$$\dot{\tilde{e}}_t = \tilde{v}\cos\tilde{e}_\theta - \tilde{v}_d[1 - \tilde{\kappa}_d\tilde{e}_n] \tag{15a}$$

$$\dot{\tilde{e}}_n = \tilde{v}\sin\tilde{e}_\theta - \tilde{v}_d\tilde{\kappa}_d\tilde{e}_t \tag{15b}$$

$$\dot{\tilde{e}}_\theta = \tilde{v}\frac{\sin\tilde{\beta}}{\lambda} + \frac{\lambda}{l}\cos^2\tilde{\beta}\left[1 + \left[\frac{l}{\lambda}\right]^2\tan^2\tilde{\beta}\right]u_1 - \tilde{v}_d\tilde{\kappa}_d \tag{15c}$$

$$\dot{\tilde{v}} = w_2\frac{1}{\cos\tilde{\beta}} + \tilde{v}\frac{\lambda}{l}\sin\tilde{\beta}\cos\tilde{\beta}\left[1 + \left[\frac{l}{\lambda}\right]^2\tan^2\tilde{\beta}\right]u_1 \tag{15d}$$

and

$$\dot{\tilde{\beta}} = \frac{\lambda}{l}\cos^2\tilde{\beta}\left[1 + \left[\frac{l}{\lambda}\right]^2\tan^2\tilde{\beta}\right]u_1. \tag{16}$$

With the introduction of the new control variables $(\tilde{w}_1, \tilde{w}_2)^T := (\dot{\tilde{e}}_\theta, \dot{\tilde{v}})^T$, we can propose the following:

Theorem 2: The control law

$$\tilde{w}_1 = -\tilde{k}_1\tilde{v}_d\left[\tilde{e}_t\frac{\cos\tilde{e}_\theta - 1}{\tilde{e}_\theta} + \tilde{e}_n\frac{\sin\tilde{e}_\theta}{\tilde{e}_\theta}\right] - \tilde{k}_4\tilde{e}_\theta \tag{17}$$

$$\tilde{w}_2 = \dot{\tilde{v}}_d - \tilde{k}_3\tilde{e}_v - \tilde{k}_1\tilde{e}_t\cos\tilde{e}_\theta - \tilde{k}_1\tilde{e}_n\sin\tilde{e}_\theta \tag{18}$$

with $\tilde{e}_v := \tilde{v} - \tilde{v}_d$, $\tilde{k}_1, \tilde{k}_3, \tilde{k}_4 > 0$ asymptotically stabilizes $[\tilde{e}_t, \tilde{e}_n, \tilde{e}_\theta, \tilde{e}_v] = 0$ of the system (15), as long as $|\tilde{\beta}| < \frac{\pi}{2}$ and $\dot{s}_d \neq 0$.

Proof: Using $\tilde{V} = (1/2)\left[\tilde{k}_1\tilde{e}_t^2 + \tilde{k}_1\tilde{e}_n^2 + \tilde{e}_\theta^2 + \tilde{e}_v^2\right]$ as a Lyapunov-function candidate, we obtain its time derivative

$$\begin{aligned}\dot{\tilde{V}} &= \tilde{k}_1\tilde{e}_t\dot{\tilde{e}}_t + \tilde{k}_1\tilde{e}_n\dot{\tilde{e}}_n + \tilde{e}_\theta\dot{\tilde{e}}_\theta + \tilde{e}_v\dot{\tilde{e}}_v \\ &= -\tilde{k}_4\tilde{e}_\theta^2 - \tilde{k}_3\tilde{e}_v^2 \leq 0\end{aligned}$$

along the lines of the calculations following (8). In order to prove asymptotical stability, we again apply[7] LaSalle's invariance theorem by letting $\tilde{S} = \{[\tilde{e}_t, \tilde{e}_n, \tilde{e}_\theta, \tilde{e}_v] \,|\, \dot{\tilde{V}} = 0\}$. With $\dot{\tilde{V}} = 0$, we conclude $\tilde{e}_\theta \equiv 0$; $\tilde{e}_v \equiv 0$, and therefore

$$\tilde{e}_v \equiv 0 \Rightarrow \dot{\tilde{v}} = \dot{\tilde{v}}_d \overset{(18)}{\Rightarrow} \tilde{e}_t = 0$$

$$\tilde{e}_\theta \equiv 0 \Rightarrow \dot{\tilde{e}}_\theta \equiv 0 \overset{(17)}{\Rightarrow} \tilde{e}_n = 0.$$

Therefore, the only solution that can stay identical in the set $\tilde{S}$ is $[\tilde{e}_t, \tilde{e}_n, \tilde{e}_\theta, \tilde{e}_v] = 0$. ■

As the proposed control law does not stabilize all states (no orientation control), it is necessary to investigate the zero dynamics of the system.

Theorem 3: The zero dynamics' trajectory of the system (15) defined by the internal dynamics of $\tilde{\beta}(t)$, when the tracking error restricted to

$$\tilde{e}_t \equiv \tilde{e}_n \equiv 0 \tag{19}$$

are bounded to $|\tilde{\beta}| < \frac{3}{4}\pi$ and $\psi(t) \to \psi_d(t)$ for $t \to \infty$ as long as $v_d > 0$

$$\max(|\kappa_d(t)|) < \frac{1}{\lambda} \tag{20}$$

and $|(\psi(t=0) - \psi_d(t=0))| \leq \frac{\pi}{2}$ holds.

Proof: With (19), (15b) yields $\tilde{e}_\theta \equiv 0$, and therefore, substituting $\dot{\tilde{\theta}}_d = \tilde{v}_d\tilde{\kappa}_d$ and (16) into (15c) calculates the zero dynamics of the system to be

$$\dot{\tilde{\beta}} = \dot{\tilde{\theta}}_d - \tilde{v}\frac{\sin\tilde{\beta}}{\lambda}. \tag{21}$$

In order to prove convergence of $\psi(t)$, we rewrite (20) as $-1 < \lambda\kappa_d < 1$ and use the change of variables

$$e_\psi = \psi - \psi_d = [\tilde{\theta}_d - \tilde{\beta}] - \psi_d \tag{22}$$

so that (21) transforms with (15a) into

$$\begin{aligned}\dot{e}_\psi &= \dot{\tilde{\theta}}_d - \dot{\tilde{\beta}} - \dot{\psi}_d = \dot{\tilde{\theta}}_d - \left[\dot{\tilde{\theta}}_d - \tilde{v}\frac{\sin\tilde{\beta}}{\lambda}\right] - \dot{\psi}_d \\ &= \tilde{v}_d\frac{\sin\tilde{\beta}}{\lambda} - v_d\kappa_d = v_d\sqrt{1 + [\lambda\kappa_d]^2}\frac{\sin\tilde{\beta}}{\lambda} - v_d\kappa_d \\ &= v_d\sqrt{1 + [\lambda\kappa_d]^2}\frac{\sin(-\psi + \tilde{\theta}_d)}{\lambda} - v_d\kappa_d \\ &= \frac{v_d}{\lambda}\sqrt{1 + [\lambda\kappa_d]^2}\sin(-\psi + \psi_d + \arctan(\lambda\kappa_d)) - v_d\kappa_d \\ &= \frac{v_d}{\lambda}\sqrt{1 + [\lambda\kappa_d]^2}(\sin(-e_\psi)\cos(\arctan(\lambda\kappa_d)) \\ &\quad + \cos(-e_\psi)\sin(\arctan(\lambda\kappa_d))) - v_d\kappa_d \\ &= \frac{v_d}{\lambda}\sqrt{1 + [\lambda\kappa_d]^2}\left[-\sin e_\psi\frac{1}{\sqrt{1 + ([\lambda\kappa_d]^2}}\right. \\ &\quad \left. + \cos e_\psi\frac{\lambda\kappa_d}{\sqrt{1 + [\lambda\kappa_d]^2}}\right] - v_d\kappa_d \\ &= -\frac{v_d}{\lambda}\left[\sin e_\psi - \lambda\kappa_d\cos e_\psi + \lambda\kappa_d\right] \\ &= -\frac{v_d}{\lambda}\left[\sin e_\psi + \lambda\kappa_d[1 - \cos e_\psi]\right]\end{aligned}$$

with the single practically relevant rest position $e_\psi = 0$. To prove convergence, we have to show that $[\sin e_\psi + \lambda\kappa_d[1 - \cos e_\psi]]$ is strictly positive (respectively, negative) for $0 < e_\psi \leq \frac{\pi}{2}$ (respectively, $-\frac{\pi}{2} \leq e_\psi < 0$). With the curvature restriction (20), we conclude that

$$\sin e_\psi + \lambda\kappa_d[1 - \cos e_\psi] \underset{(<)}{>} \sin e_\psi \underset{(+)}{(-)} [1 - \cos e_\psi] \underset{(\leq)}{\geq} 0.$$

[7] Notice that the closed-loop system defined by (15) and the proposed control law in (17) and (18) is autonomous and, in particular, not influenced by $\tilde{\beta}$.

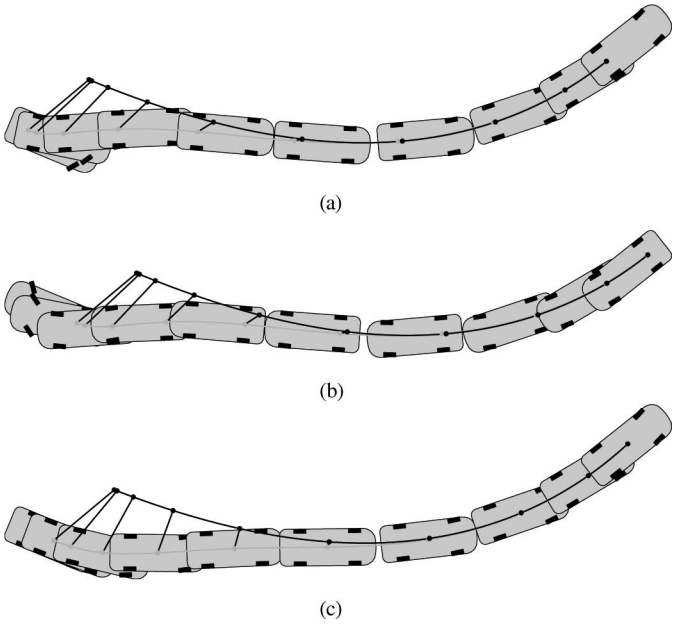

Fig. 4. Simulation results with large initial errors. (a) Forward trajectory tracking with orientation control. (b) Backward trajectory tracking with orientation control. (c) Forward trajectory tracking without orientation control.

The latter step can be verified by squaring both sides of the equivalent inequality $\sin e_\psi \underset{(-)}{\overset{+}{}} \cos e_\psi \underset{(\leq)}{\overset{\geq}{}} 1 \underset{(-)}{\overset{+}{}} 1$, which proves true as $1 \underset{(-)}{\overset{+}{}} \sin(2e_\psi) \geq 1$.

Solving (22) for $\tilde{\beta}$, with $\tilde{\theta}_d = \psi_d + \arctan(\lambda\kappa_d)$, we can finally conclude that

$$|\tilde{\beta}| = |-e_\psi - \arctan(\lambda\kappa_d)| < \frac{\pi}{2} + \frac{\pi}{4} = \frac{3}{4}\pi. \qquad \blacksquare$$

Obviously, the zero dynamics become unstable if v_d becomes negative. This is sometimes referred to as "jack-knife" effect, since the orientation error increases rapidly during backward driving.

Notice that the restrictions on δ, $\tilde{\beta}$, e_ψ, and κ_d in the proposed control laws of this section are irrelevant in practice: From the last equation of (14), we know that $|\tilde{\beta}| < \frac{\pi}{2}$ and $|\delta| < \frac{\pi}{2}$ are equivalent. Due to the steering-angle saturation, however, this condition will always be met. Furthermore, large orientation errors such as $|e_\psi| > \frac{\pi}{2}$ can be prevented as well as the steering-angle saturation by an error-triggered-replanning strategy. As it also has to take the limited turning radius of the car into account, (20) is no additional restriction on the maximum feasible curvature.

E. Simulative Validation of the Idealized-Feedback System

The simulation of the idealized-closed-loop system (no noise, disturbances, or saturation) for forward and backward tracking of a reference trajectory are given in Fig. 4. It illustrates the asymptotical[8] stabilization of the large initial position errors, as assured by the applied control-design method, which encourage us for the practical implementation in the following section. However, the simulation already gives away that the feedback law with orientation control [regardless of the direction, see Fig. 4 (a) and (b)] requires higher steering amplitudes in order to induce the same centric error decays $\tilde{e}_n(t)$ and $\tilde{e}_t(t)$ than the one without orientation control [see Fig. 4(c)].

[8]Down to a numerical noise level of less than 10^{-4} m.

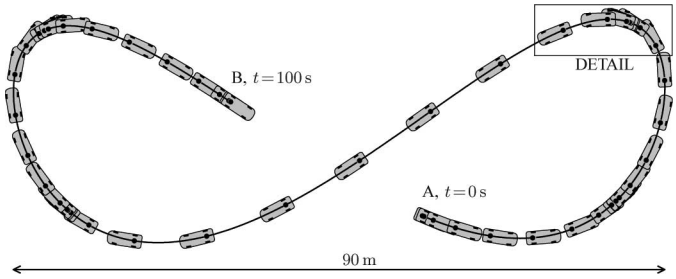

Fig. 5. Visualization of closed-loop test run from A to B.

V. Practical Implementation and Results

In this section, we compare the two control algorithms by means of our full-scale experimental vehicle [5] on a tarred, slightly uneven test site ($49°1'22$ N, $8°25'54$ E). The Volkswagen Passat is equipped with automatic transmission, by-wire steering, throttle, and braking, which leads, with the computers and sensors, to an extra load of 650 kg. The controllers are implemented in a quasi-continuous fashion (1.0 kHz) on a dSpace real-time environment, and the self-localization (position and orientation) is based on a GPS inertial-navigation system supported by odometry and OmniSTAR [15].

As the turning of the (sensorless) front wheels is carried out by a motorized steering column, the static characteristic $\delta(\delta_c)$ between the effective steering angle δ and the steering column angle δ_c needs to be accounted for. In our experience, significantly better results can be achieved during sharp turns if the minor nonlinearity of the steering kinematics is incorporated. It can be best determined experimentally by an automated evaluation of different values of δ_c and the resulting curvatures κ_δ of the rear axis' GPS-trace, according to $\delta(\delta_c) = \arctan(l\kappa_\delta(\delta_c))$. As a matter of fact, the resulting kinematics differ noticeably between forward and backward driving, which we attribute to the rubber-mounting parts giving, depending on the driving direction. As the VW Passat is front-wheel driven, we take $\gamma = 1.0$, and as soon as the brakes engage, we switch to the estimated brake-balance value of $\gamma = 0.75$. In order to convert the calculated longitudinal forces to throttle position and brake pressure, a feedback-linearizing [6] split-range controller [16] was implemented, which accounts for the rolling and air resistance, the engine characteristics, as well as the ratio of the engaged gear. All required parameters can be accurately determined by standard measurements such as weighing (mass and center of gravity) and analyzing step responses (moment of inertia, engine and brake characteristics, as well as resistances).

In order to eliminate the influence of trajectory planning on the tracking results, we substitute the planning level of the autonomous system by an offline-generated velocity adjusted Lissajous trajectory,[9] as depicted in Fig. 5, which results in a stop-and-go typical maneuver with intermediate halts of 1.0 s that occur every 20–25 s. Notice that the chosen trajectory represents with its permanent curvature and velocity changes a fairly generic one and that forward and backward sections between intermediate stops can be combined (however, this is not done in the test run) in order to realize K-turn like maneuvers (U-turns with two shifts in direction) so that they are not demonstrated here separately.

At test start, this desired trajectory is initialized by launching directly from the rear-axis center with v_d =0.0 m/s, while the vehicle has, in turn, engaged the desired gear and waits with aligned steering so that no initial errors occur. This has been done because there is no need for

[9]Known among others from oscilloscopes

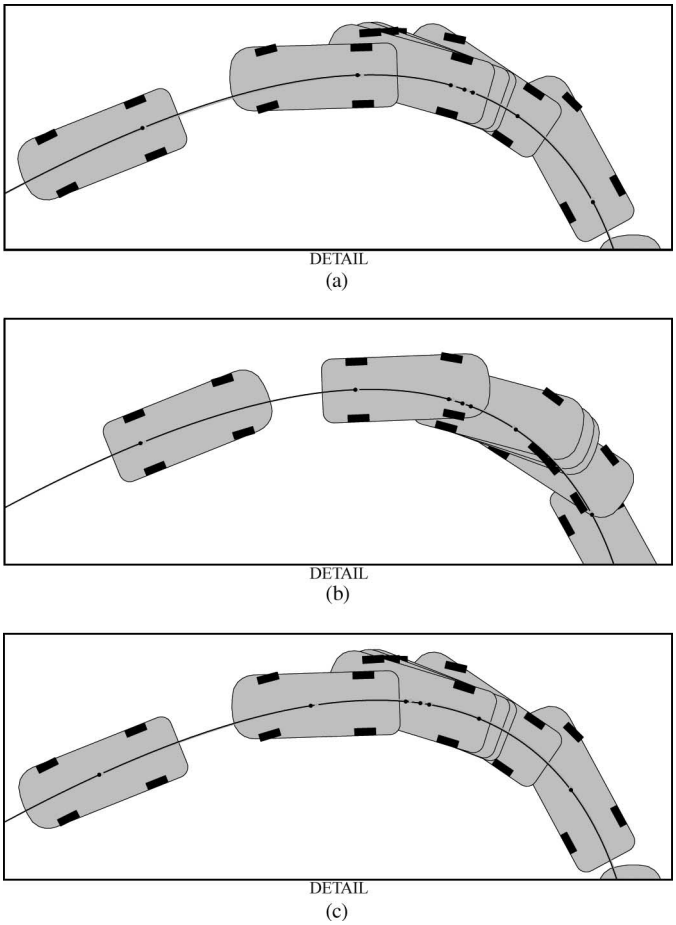

Fig. 6. Detailed views of Fig. 5 for the different tracking controllers. (a) Forward trajectory tracking with orientation control. (b) Backward trajectory tracking with orientation control. (c) Forward trajectory tracking without orientation control.

an autonomous vehicle to start with an initial error as the trajectories are normally generated online.

The test results for forward and backward orientation-controlling tracking just as forward tracking without orientation control can be seen in Fig. 7, as well as the detailed views of the movement in time-equidistant stop-motion in Fig. 6. In each plot, we assume "ground truth" of the self-localization. Even though the desired trajectory is designed with permanent velocity changes and curvatures close to the minimum turn radius of the test vehicle, the centric-tracking errors stay during numerous consecutive test runs for all three controllers below 7 cm in the lateral direction, 22 cm in longitudinal direction, and 1.2° in orientation.

VI. Discussion

According to the previous section, the two control strategies appear to perform comparably well. However, the feedback law without orientation control requires less steering effort $\dot{\delta}(t)$ (smoothness of δ in Fig. 7) and smaller amplitudes[10] of δ in order to deliver the same performance as the feedback law with orientation control. Besides that, they both demonstrate the same high accuracy in the lateral direction and

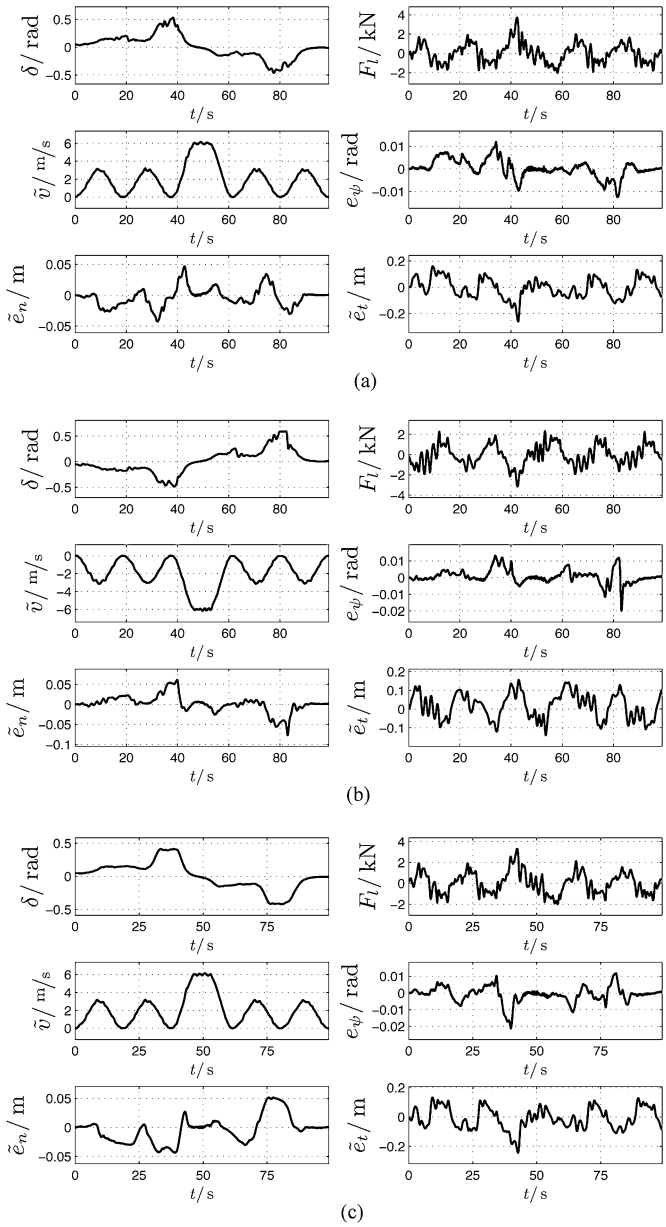

Fig. 7. Tracking performance of practical test run. (a) Forward trajectory tracking with orientation control. (b) Backward trajectory tracking with orientation control. (c) Forward trajectory tracking without orientation control.

orientation. The longitudinal error is noticeably larger but still acceptable, since safety clearances ahead and behind the car can be chosen bigger than those on the sides without jeopardizing the traffic flow.[11]

The presence of the lateral errors in the test runs are attributed to the GPS drift[12] and the play in the steering linkage, whereas the longitudinal errors are mainly caused by the unmodeled gear-switching operation of the automatic transmission at approximately 4.0 m/s (except for backward driving, where the longitudinal-tracking performance is better), the underlying (unmodeled)-idling control, the neglected lag

[10]Due to smaller steering amplitudes of a control law, the planning level can take advantage of sharper turns as the danger of steering-angle saturation is reduced.

[11]A lateral deviation of half a meter from the safe traffic corridor may easily lead to a sideswipe of a passing car, whereas the same deviation in the longitudinal direction would only be noticed during static-parking maneuvers, at which classical path-stabilization strategies should be chosen over dynamic trajectory concepts anyway.

[12]GPS–RMS values are about 10 cm for position and 0.1° for orientation.

of the brake booster and the throttle control, as well as the GPS drift. All these negative effects (except for the GPS measurement) could be significantly reduced by a better knowledge of the vehicle's hardware and its revision in favor of the autonomous application.

As can be deduced from the linearized closed-loop behavior, both the feedback law with and without orientation control avoid the singularity at $v = 0$ by assuring convergence in the lateral direction simply over the covered arc-length analogously to "time-scaling" to provide a smooth, pleasant ride to the occupants (see Fig. 6). This means when $\dot{s}_d$ becomes zero (excluded from the proofs), the control laws "patiently freeze" the current lateral error (the system is during the dwell only stable). However, the longitudinal error, as well as the steering angle, are in either case stabilized "in t," which is attributed to the fact that in both the law (6) and (7) and the law (17) and (18), the respective feedback gains neither depend on the actual nor on the desired velocity. This, in turn, means that the associated error states do not drift during (arbitrarily) long stops (such as in the beginning and the end of the test run), even when $\dot{s}_d = 0$.

As bigger lateral errors become involved (caused by momentary, safety-related manual-steering interference during system failure, testing of new algorithms, which leads to discontinuities of the desired trajectory, or GPS position jumps and does not occur in the test run), the tracking law with orientation control shows wind-up phenomena. They arise from the steering-rate saturation of the actuator, which can easily be reproduced by simulation. By contrast, the feedback law without orientation control is by far better natured and does not show these phenomena. This is not surprising since course corrections are directly carried out by the orientation of the steering and not by the heading of the whole car, as in the case of the tracking law with orientation control. The feedback noninfluenceable zero dynamics are stable during forward driving and converge sufficiently fast so that the choice of $\lambda \approx (l/2)$ seems to be a good one. Furthermore, the feedback law without orientation control operates adequately at somewhat higher speeds, where the kinematic model loses its validity.

VII. Conclusion

In order to handle dynamic street scenarios with a full-scale autonomous road vehicle, we have proposed two solutions to the trajectory-tracking problem. The derived Lyapunov-based control laws perform quite accurately and complement one another, which we illustrated by means of a real-time implementation on a test vehicle. While the tracking law with orientation control alone allows for backward driving, the feedback law without orientation control generates much smoother steering inputs and does not tend to wind-up phenomena so quickly during forward maneuvering.

As both controllers are based on the kinematic one-track model, stability is only guaranteed up to moderate velocities where the pure rolling assumption holds. To extend the control range to higher speeds is, therefore, an issue for future research. We hope that *AnnieWAY* will so be well prepared for another, maybe even more realistic, *Urban Challenge*.

References

[1] A. Aguiar and J. Hespanha, "Trajectory-tracking and path-following of underactuated autonomous vehicles with parametric modeling uncertainty," *IEEE Trans. Automat. Control*, vol. 52, no. 8, pp. 1362–1379, Aug. 2007.

[2] G. Campion and W. Chung, "Wheeled Robots," in *Springer Handbook of Robotics*. New York: Springer-Verlag, 2008, pp. 391–410.

[3] L. Fletcher, S. Teller, E. Olson, D. Moore, Y. Kuwata, J. How, J. Leonard, I. Miller, M. Campbell, D. Huttenlocher, A. Nathan, and F.-R. Kline, "The MIT-Cornell collision and why it happened," *J. Field Robot.*, vol. 25, no. 10, pp. 775–807, 2008.

[4] M. Fliess, J. Lévine, P. Martin, and P. Rouchon, "Flatness and defect of non-linear systems: Introductory theory and examples," *Int. J. Control*, vol. 61, no. 6, pp. 1327–1361, 1995.

[5] S. Kammel, J. Ziegler, B. Pitzer, M. Werling, T. Gindele, D. Jagszent, J. Schröder, M. Thuy, M. Goebl, F. v. Hundelshausen, O. Pink, C. Freese, and C. Stiller, "Team AnnieWAY's autonomous system for the DARPA Urban Challenge 2007," *J. Field Robot.*, vol. 25, no. 9, pp. 615–639, 2008.

[6] M. Krstic, P. V. Kokotovic, and I. Kanellakopoulos, *Nonlinear and Adaptive Control Design*. New York: Wiley, 1995.

[7] P. Martin, P. Rouchon, and J. Rudolph, "Invariant tracking," *Control, Optim. Calculus Variations*, vol. 10, no. 1, pp. 1–13, Jan. 2004.

[8] P. Morin and C. Samson, "Trajectory tracking for nonholonomic vehicles," *Lecture Notes in Control and Information Science*, vol. 335, pp. 3–23, 2006.

[9] P. Morin and C. Samson, "Motion control of wheeled mobile robots," in *Springer Handbook of Robotics*. New York: Springer-Verlag, 2008, pp. 799–826.

[10] P. Morin and C. Samson, "Control of nonholonomic mobile robots based on the transverse function approach," *IEEE Trans. Robot.*, vol. 25, no. 5, pp. 1058–1073, Oct. 2009.

[11] P. Rouchon and J. Rudolph, "Invariant tracking and stabilization: Problem formulation and examples," in *Lecture Notes in Control and Information Sciences*, New York, Springer-Verlag, 1999, pp. 261–273.

[12] M. Sampei and K. Furuta, "On time scaling for nonlinear systems: Application to linearization," *IEEE Trans. Automat. Control*, vol. AC-31, no. 5, pp. 459–462, May 1986.

[13] C. Samson, "Control of chained systems application to path following and time-varying point-stabilization of mobile robots," *IEEE Trans. Automat. Control*, vol. 40, no. 1, pp. 64–77, Jan. 1995.

[14] M. Werling, T. Gindele, D. Jagszent, and L. Gröll, "A robust algorithm for handling moving traffic in urban scenarios," in *Proc. IEEE Intell. Veh. Symp.*, Eindhoven, The Netherlands, 2008, pp. 1108–1112.

[15] M. Werling, M. Goebl, O. Pink, and C. Stiller, "A hardware and software framework for cognitive automobiles," in *Proc. IEEE Intell. Veh. Symp.*, Eindhoven, The Netherlands, 2008, pp. 1080–1085.

[16] M. Werling, L. Gröll, and G. Bretthauer, "A multi controller for testing full-autonomous driving," *at-Automatisierungstechnik*, vol. 11, pp. 585–591, 2008.